Free Radical Biology and Medicine 97 (2016) 223–235

Contents lists available at ScienceDirect

Free Radical Biology and Medicine

journal homepage: www.elsevier.com/locate/freeradbiomed

Original article

# 9-Norbornyl-6-chloropurine (NCP) induces cell death through GSH depletion-associated ER stress and mitochondrial dysfunction

Pavla Plačková [a], Michal Šála [a], Markéta Šmídková [a], Milan Dejmek [a], Hubert Hřebabecký [a], Radim Nencka [a], Hendrik-Jan Thibaut [b], Johan Neyts [b], Helena Mertlíková-Kaiserová [a,*]

[a] Institute of Organic Chemistry and Biochemistry, Academy of Sciences of the Czech Republic, v.v.i., 166 10 Prague 6, Czech Republic
[b] Rega Institute for Medical Research, KU Leuven, Minderbroedersstraat 10, BE-3000 Leuven, Belgium

ARTICLE INFO

*Article history:*
Received 8 February 2016
Received in revised form
3 June 2016
Accepted 6 June 2016
Available online 7 June 2016

*Keywords:*
Norbornylpurines
Glutathione
Apoptosis
Unfolded protein response
Mitochondrial membrane potential
Reactive oxygen species
Nrf-2

ABSTRACT

9-Norbornyl-6-chloropurine (NCP) is a representative of a series of antienteroviral bicycle derivatives with selective cytotoxicity towards leukemia cell lines. In this work we explored the mechanism of the antileukemic activity of NCP in T-cell lymphoblast cells (CCRF-CEM). Specifically, we searched for a potential link between its ability to induce cell death on the one hand and to modulate intracellular glutathione (GSH) that is necessary to its metabolic transformation via glutathione-*S*-transferase on the other hand. We have observed that GSH levels decreased rapidly in NCP-treated cells. Despite a complete regeneration following 24 h of incubation with NCP, this profound drop in cellular GSH content triggered ER stress, ROS production and lipid peroxidation leading to the loss of mitochondrial membrane potential (MMP). These events induced concentration-dependent cell cycle arrest in G2/M phase and apoptosis. Both MMP loss and apoptosis were reversed by sulfhydryl-containing compounds (GSH, *N*-acetyl-L-cysteine). Furthermore, we have also shown that NCP-induced GSH decrease activated the Nrf2 pathway and its downstream targets NAD(P)H:quinone oxidoreductase (NQO-1) and glutamate cysteine ligase modifier subunit (GCLm), thus explaining the fast restoration of GSH pool and ROS decrease. Importantly, we confirmed that the cell death-inducing properties of the compounds were co-dependent on their ability to diminish cellular GSH level by analyzing the relationships between the GSH-depleting potency and cytotoxicity in a series of other norbornylpurine analogs. Altogether, the results demonstrated that in CCRF-CEM cells NCP triggered apoptosis through GSH depletion-associated oxidative and ER stress and mitochondrial depolarization.



## 1. Introduction

9-Norbornylpurine derivatives are a class of in-house synthesized compounds originally developed as antienteroviral drugs with enhanced activity against Coxsackievirus B3 [1–5].

9-Norbornyl-6-chloropurine (NCP, compound **1**, Fig. 1) represents the prototype structure of the series and has been found to possess significant cytostatic activity, particularly towards human leukemia cell lines. This suggested the potential of these compounds as prospective anticancer drugs as well. Although 9-norbornylpurines could be regarded as carbocyclic nucleoside analogs, our previous *in vitro* experiments with NCP revealed that they do not behave as nucleoside analogs, but rather as substituted nucleobases. The lipophilic norbornane moiety in fact does not mimic the sugar but provides the compounds with the advantageous pharmacokinetic properties as exemplified by excellent membrane permeability in intracellular transport assays in CCRF-CEM (T-lymphoblast) cells as well as in the transepithelial Caco-2 assay [6]. Previously, we have also demonstrated the essential role of glutathione (GSH) in the metabolic transformation of NCP to polar conjugates (NCP-GS) in CCRF-CEM cells. The reaction was found to be strictly dependent on glutathione-*S*-transferase (GST) activity and cellular GSH (the absence of metabolite formation in BSO-treated cells). The conjugates were readily formed and excreted from the cells. They also exhibited lower toxicity compared

*Abbreviations:* NCP, 9-norbornyl-6-chloropurine; GST, glutathione-*S*-transferase; GSH, L-glutathione reduced; MMP, mitochondrial membrane potential; GR, glutathione reductase; PI, propidium iodide; 4-PBA, sodium phenylbutyrate; QUER, quercetin; ALLO, allopurinol; ABT, 1-aminobenzotriazole; CCCP, carbonyl cyanide 3-chlorophenylhydrazone; CAPE, caffeic acid phenethyl ester; MDA, 1,1,3,3-tetraethoxypropane; DPI, diphenyleneiodonium chloride; TBA, 2-thiobarbituric acid; EDTA, ethylenediaminetetraacetic acid; TFA, trifluoroacetic acid; GSSG, L-glutathione oxidized; SA, sulfosalicylic acid; CDNB, 1-chloro, 2,4-dinitrobenzene; LO, lipoxygenase

* Corresponding author.
*E-mail address:* mertlikova@uochb.cas.cz (H. Mertlíková-Kaiserová).

http://dx.doi.org/10.1016/j.freeradbiomed.2016.06.004
0891-5849/

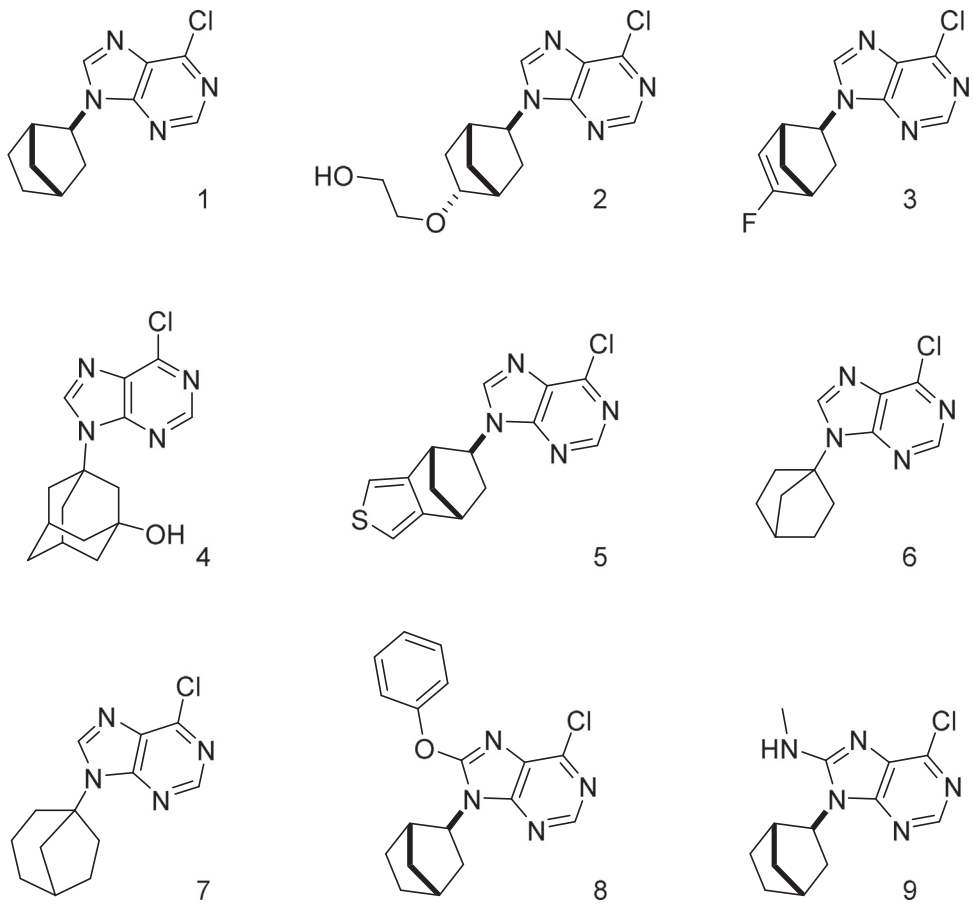


**Fig. 1.** Structures of substituted 9-norbornyl-6-chloropurines. 1: 9-[(1*R**, 2*R**, 4*S**)-bicyclo[2.2.1]hept-2-yl]-6-chloro-9*H*-purine (NCP), 2: 2-(((1*R**, 2*R**, 4*R**, 5*S**)-5-(6-chloro-9*H*-purin-9-yl)bicyclo[2.2.1]heptan-2-yl)oxy)ethanol, 3: 6-chloro-9-((1*R**, 2*S**, 4*R**)-5-fluorobicyclo[2.2.1]hept-5-en-2-yl)-9*H*-purine, 4: (1*s*, 3*r*, 5*R**, 7*S**)-3-(6-chloro-9*H*-purin-9-yl)adamantan-1-ol, 5: 6-chloro-9-[(1*R**, 7*R**, 8*S**)-4-thiatricyclo[5.2.1.02,6]deca- 2,5-dien-8-yl-9*H*-purine, 6: 9-(bicyclo[2.2.1]heptan-1-yl)-6-chloro-9*H*-purine, 7: 9-(bicyclo[3.2.1]octan-1-yl)-6-chloro-9*H*-purine, 8: 9-((1*S**, 2*S**, 4*R**)-bicyclo[2.2.1]heptan-2-yl)-6-chloro-8-phenoxy-9*H*-purine 9: 9-((1*S**, 2*S**, 4*R**)-bicyclo[2.2.1]heptan-2-yl)-6-chloro-*N*-methyl-9*H*-purin-8-amine.

to NCP [7]. Regarding to the above mentioned facts, it is of interest whether the cytotoxic effects of NCP are directly linked to its ability to cause GSH depletion (resulting from NCP metabolism) and consequent oxidative stress or whether a distinct mechanism is involved.

Although physiological level of reactive oxygen species (ROS) serves for the signalling and normal functioning in the cells, cancer cells, compared to normal cells, are under increased oxidative stress [8]. This may provide an opportunity to kill cancer cells based on their vulnerability to further ROS increase. The natural source of ROS in cells are enzymatic reactions (e.g., mitochondrial respiratory chain reactions, arachidonic acid pathway, cytochrome P450 family and those involving glucose oxidase, amino acid oxidase, xanthine oxidase, NADP/NADPH oxidase or NO synthases) [9]. These reactions take place in mitochondria, endoplasmic reticulum (ER), plasma membrane and cytosol [10]. ROS formation is balanced by a highly efficient system of antioxidants, including both enzymatic and nonenzymatic pathways [11]. GSH serves as a major regulator of the cellular redox homeostasis and protects the cell against ROS and electrophiles. As a donor of –SH group, it acts either as a direct antioxidant or indirectly as a cofactor of phase II enzymes, such as GST [12]. GSH depletion, especially that of its mitochondrial pool, has been described to induce apoptotic cell death [13].

The ER represents a major protein folding site in the cell. The accumulation of incorrectly folded proteins triggers ER stress and activation of the unfolded protein response (UPR). The UPR comprises three parallel signaling pathway: PKR-like ER kinase (PERK), eukaryotic translation initiation factor 2α (eIF2α), inositol-requiring protein 1α (IRE1α) and activating transcription factor 6α (ATF6α). Because the UPR employs both protective and apoptotic effects on cell survival upon ER stress, UPR activation may facilitate, as well as suppress, malignant transformation [14]. Many studies suggest that ER regulates apoptosis both by sensitizing mitochondria to a death stimulus and by initiating cell death signals of its own [15,16]. ER stress has also been recognized as a mechanism leading to tumor cell death following chemotherapeutics. ROS have recently emerged as crucial regulators of ER function [11] as oxidative stress and ER stress are frequently observed together. ROS-mediated UPR may lead to apoptosis activation via PERK, which has been reported to be involved in mitochondria-ER crosstalk [17]. Mitochondria are one of particularly affected organelles in the apoptotic process where BCL-2 family proteins are central regulators of apoptosis [18]. Alterations in mitochondrial physiology, such as dissipation of the inner membrane potential and/or release of intermembrane proteins, have been described in many apoptotic responses [19]. The mitochondrial dysfunction is connected with several human diseases, while, on the other hand, mitochondria represent suitable targets for activating specific killing of cancer cells [20,21].

The transcriptional activation of the antioxidant response elements (ARE), mediated primarily by nuclear factor E2-related factor 2 (Nrf2), is a major mechanism in cellular defense against oxidative and electrophilic stress. Nfr2 pathway is one of the antioxidant mechanisms, which can also be activated in response to ER stress [22]. The transcription factor Nrf2 is required for the

expression of glutamate cysteine ligase catalytic subunit (GCLc) and glutamate cysteine ligase modifier subunit (GCLm), which are necessary for GSH biosynthesis. Nrf2 also regulates expression of other cellular detoxifying enzymes, e.g. NAD(P)H:dehydrogenase, quinone 1 (NQO1) [23].

The goal of this study was to elucidate the mechanism by which NCP induces apoptosis in leukemia (CCRF-CEM) cells. Specifically, we aimed to investigate the role of GSH and oxidative stress signaling and its consequences such as ER stress and mitochondrial dysfunction in NCP-induced cell death.

## 2. Material and methods

### 2.1. Materials

NCP was synthesized as described previously [24]. Stock solutions were prepared by the dissolving of the compound in DMSO at 50 mM concentration. Allopurinol (ALLO), 1-aminobenzotriazole (ABT), BCA kit, streptomycin, penicillin G, PBS, RPMI-1640 medium, RPMI-1640 Dutch modification medium, fetal calf serum, carbonyl cyanide 3-chlorophenylhydrazone (CCCP), caffeic acid phenethyl ester (CAPE) diphenyleneiodonium chloride (DPI), sodium phenylbutyrate (4-PBA), 1,1,3,3-tetraethoxypropane (MDA), ethylenediaminetetraacetic acid (EDTA), 2-thiobarbituric acid (TBA), trifluoroacetic acid (TFA), L-glutathione reduced (GSH), L-glutathione oxidized (GSSG), RNaseA, sulfosalicylic acid (SA), quercetin (QUER) 5,5′-dithiobis(2-nitrobenzoic acid) (DTNB), β-NADPH, ATP, staurosporine, 1-chloro-2,4-dinitrobenzene (CDNB), acetonitrile, methanol, protease and phosphatase inhibitor cocktail, glutathione reductase (GR) from baker's yeast (E.C 1.6.4.2, 500 UN), CHAPS and monoclonal anti-β-actin antibody were purchased from Sigma–Aldrich (St. Louis, MO, USA). CM-$H_2$DCFDA (General Oxidative Stress Indicator), JC-1 dye (Mitochondrial Membrane Potential Probe), Dead Cell Apoptosis Kit with Annexin V Alexa Fluor® 488 & Propidium Iodide (PI) and MitoSOX™ Red Mitochondrial Superoxide Indicator were purchased from ThermoFisher Scientific (Waltham, MA USA). CaspACE™ FITC-VAD-FMK In Situ Marker was purchased from Promega (Madison, WI, USA). Salts for buffer preparations were purchased from Serva (Heidelberg, Germany). Monoclonal anti-Nrf2, -NQO-1, -GCLm, -p-eIF2α (phosphorylated form), histone H3 (H3) and -p-IRE1 (phosphorylated form) antibodies were purchased from Cell Signaling Technology, Inc. (Danvers, MA, USA).

### 2.2. Cell culture

CCRF-CEM and BGM cells (ATCC®, UK) were grown in RPMI-1640 and Eagle's MEM medium, respectively, supplemented with 10% (v/v) fetal calf serum, 200 μg/ml of streptomycin, 200 U/ml of penicillin G and 4 mM glutamine. They were cultured under a humidified atmosphere containing 5% $CO_2$ at 37 °C. Unless otherwise indicated, cells were seeded into the 6-well plates at a density from $6 \times 10^4$ (for 72 h incubation) to $3 \times 10^5$ (for 24 h incubation) cells per well and left to rest overnight. 10–30 μM NCP was then added and incubated for up to 72 h.

### 2.3. Cell cycle analysis

$1 \times 10^6$ NCP-treated cells were washed thoroughly with PBS ($250 \times g$ for 5 min) and resuspended in 0.5 ml of ice-cold PBS. 4.5 ml of ice-cold 80% ethanol was then added drop wise while vortexing, fixed on ice for 30 min and centrifuged at $250 \times g$ for 5 min at 4 °C. Pelleted cells were resuspended in 0.5 ml of PBS containing PI (0.1 mg/ml), RNaseA (8.7 mg/ml) and Triton-X 100 (0.1%) and incubated for 1 h. The cellular DNA content was determined by FACSFortessa (BD Biosciences, San Jose, CA). The data were plotted as histograms and the distribution of the cell cycle phases was analyzed using ModFit LT 3.0 (Verity Software House, Topsham, ME).

### 2.4. Apoptosis determination

The phosphatidylserine externalization in the apoptotic cells was quantified using an Alexa Fluor 488 Annexin V/Dead cell apoptosis kit (Invitrogen (Carlsbad, CA, USA) according to the manufacturer's instructions. Briefly, $1 \times 10^6$ cells treated with NCP or 1 μM staurosporine were washed thoroughly with PBS ($250 \times g$ for 5 min) and resuspended in 0.1 ml of 1 × annexin-binding buffer. Then, 5 μl of Alexa Fluor 488 Annexin V and 1 μl of PI (100 μg/mL) were added to 100 μl of the cell suspension. Cells were gently mixed, and incubated for 15 min at room temperature in the dark. After that, 400 μl of 1 × annexin-binding buffer was added to each tube, and samples were analyzed by flow cytometry using FACSFortessa Cell Sorter (BD Biosciences, San Jose, CA USA). Annexin $V^+$ $PI^-$ cells represented an early apoptotic population. Annexin $V^+$ $PI^+$ cells represented either late apoptotic or secondary necrotic populations.

The activation of caspases in NCP-treated samples was analyzed by means CaspACE™ In Situ Marker. $1 \times 10^6$ cells were washed thoroughly with PBS ($250 \times g$ for 5 min) and resuspended in 0.5 ml of 10 μM CaspACE solution in PBS. After 20 min at room temperature in the dark, the samples were centrifuged at $250 \times g$ for 5 min, resuspended in 0.5 ml of HBSS and analyzed by FACS.

### 2.5. Glutathione determination

Total GSH content was determined according to Rahman et al. [25]. CCRF-CEM and BGM cells were lysed in ice-cold extraction buffer containing 0.1% Triton-X 100 and 0.6% SA in water and centrifuged at $3000 \times g$ for 4 min at 4 °C. 20 μl of the supernatant or standard solution (GSH and GSSG) was mixed with 120 μl of DTNB and GR (1:1) in a 96-well plate. After 30 s, 6 μl of β-NADPH was added and measured immediately at 412 nm using an Infinite M1000 plate reader (Tecan Systems Inc., San Jose, CA, USA). Absorbance was recorded every 15 s for 10 min.

### 2.6. Detection of reactive oxygen species (ROS)

CCRF-CEM cells were treated with NCP as described in 2.2 or alternatively, the cells were pre-incubated (0.5 h) with the inhibitors –10 μM CCCP (the uncoupler of mitochondrial respiratory chain), 2 mM DPI (the inhibitor of NADPH-oxidase), 0.5 mM ALLO (the inhibitor of xanthine/xanthine oxidase), 0.25 mM ABT (the inhibitor of CYP450), 10 μM CAPE (the inhibitor of lipoxygenase) and 5 mM 4-PBA (the inhibitor of ER-stress) or antioxidants 3 mM GSH, 3 mM NAC and 10 μM QUER prior to the addition of 20 μM NCP. After the treatment, $1 \times 10^6$ cells were washed thoroughly with PBS ($250 \times g$ for 5 min), resuspended in 0.5 ml of 1 μM CM-$H_2$DCF-DA solution in HBSS (for general ROS detection) and incubated for 1 h in the dark at 37 °C or in 0.5 ml of 3.5 μM MitoSOX™ solution in HBSS (for mitochondrial superoxide detection) for 0.5 h in the dark at RT and then washed thoroughly with PBS ($250 \times g$ for 5 min). Pelleted cells were resuspended in 0.5 ml of HBSS and analyzed by FACS.

### 2.7. Determination of lipid peroxidation

50 μl of cell suspension ($1 \times 10^6$ cells/ml) in PBS or MDA standard solutions was mixed with 450 μl of TBA reagent (12 mM TBA, 0.32 M $H_3PO_4$, EDTA 0.01%, 1.35 mg/ml BHT in EtOH), incubated for 1 h at 99 °C and chilled on ice. Chilled samples were extracted to

*n*-butanol by vortexing and centrifuged at 1000 × *g* for 1 min. The organic phase was injected onto a Nova-Pack C18 HPLC column (3.9 × 15 mm, Waters) and separated using the Waters Alliance HT HPLC system with fluorescent detection. The mobile phase consisted of 35% methanol and 65% water with 0.05% TFA. The flow rate was 0.7 ml/min. The fluorescence intensity was recorded at $\lambda_{ex}$=532 nm and $\lambda_{em}$=553 nm.

### 2.8. Protein extraction and Western blotting

NCP-treated cells were washed with PBS (250 × *g* for 5 min) and lysed by ice-cold RIPA buffer ($10^7$ cells/150 μl) containing protease and phosphatase inhibitors for 30 min on ice and centrifuged at 14,000 × *g* for 30 min at 4 °C. The supernatant contained whole cell extract which was used for NQO-1, GCLm and LO activity assay. Alternatively, cells were washed with PBS (250 × *g* for 5 min) and re-suspended in ice-cold hypotonic buffer (10 mM HEPES pH 7.5, 2 mM $MgCl_2$, 25 mM KCl and fresh 1 mM DTT and protease and phosphatase inhibitor cocktail) at 5 × $10^7$ cells/ml. After 30 min NP-40 was added to 0.5% concentration, mixed gently and centrifuged at 1000 × *g* for 15 min at 4 °C. The supernatant (cytosol) was removed. The pellet (nuclei) was washed with ice cold hypotonic buffer N (10 mM HEPES pH 7.5, 2 mM $MgCl_2$, 25 mM KCl, 250 mM sucrose and fresh 1 mM DTT, and protease and phosphatase inhibitor cocktail) and centrifuged at 1000 × *g* for 15 min at 4 °C. Isolated nuclei were then lysed as the whole cellular extract and it was used for Nrf-2 detection.

Membrane proteins were isolated as follows: cells were washed with PBS and suspended in ice cold lysis buffer (20 mM HEPES pH 7.0, 25 mM KCl, 25% glycerol, 2 mM EDTA, 20 mM CHAPS) at 5 × $10^7$ cells/ml on ice for 30 min and centrifuged at 14,000 × *g* for 30 min at 4 °C. The supernatant contained membrane protein which was used for p-eIE2α and p-IRE1 detection.

Microsomal fraction was isolated as follows: cells were washed with PBS (250 × *g* for 5 min) and re-suspended in ice-cold phosphate buffer (0.1 M, pH=7.4) containing 20% glycerol at 1 × $10^7$ cells/ml. Following the ultrasonic lysis, the lysate was centrifuged at 20,000 × *g* for 15 min at 4 °C. The supernatant was centrifuged again at 105,000 × *g* for 90 min at 4 °C. The supernatant (cytosol) was removed and the pellet (microsomal fraction) was re-suspended in ice-cold phosphate buffer (0.1 M, pH=7.4) containing 20% glycerol (450 μl per sample). Cytosolic and microsomal fractions were used for GST activity and NCP-metabolism evaluation.

The protein content in each sample was determined using the BCA kit according to the protocols provided by the manufacture.

30 μg of protein was then loaded per well on polyacrylamide gel, electrophoresed and electroblotted onto a PVDF membrane (Merck, USA). Then, the membranes were blocked in 5% non-fat dry milk in TBS containing 0.05% of Tween 20 and probed with specific antibodies and appropriate HRP-conjugated secondary antibodies. SuperSignal® West Femto Maximum Sensitivity Chemiluminescent Substrate (Pierce, Waltham, MA USA) was used for signal detection by CCD camera. Densitometric analysis of blots was performed by Quantity One® 1-D analysis software (Bio-Rad, Hercules, CA, USA).

### 2.9. Detection of mitochondrial membrane potential (MMP)

CCRF-CEM cells were treated with NCP as described in 2.2 or alternatively, the cells were pre-incubated (0.5 h) with 10 μM 4-PBA, 3 mM GSH and 3 mM NAC prior to the addition of 20 μM NCP. After the treatment, 1 × $10^6$ cells were incubated with 0.5 ml of 2.5 μg/ml JC-1 solution in HBSS for 0.5 h in the dark at 37 °C and then centrifuged at 250 × *g* for 5 min. Pelleted cells were re-suspended in 0.5 ml of HBSS and analyzed by FACS.

### 2.10. ATP determination

Total ATP content was determined using CellTiter-Glo® Luminescent Cell Viability Assay kit (Madison, WI, USA) according to the protocols provided by the manufactures. Briefly, NCP-treated cells were resuspended in HBSS solution and seeded in a 96-well plate at a density of 2 × $10^5$ cells per well (50 μl). After that, 50 μl of CellTiter-Glo® solution was added to cell suspensions or ATP standard solutions, incubated for 2 min at room temperature in the dark while constantly mixing the sample and then incubated for further 10 min to stabilize luminescent signal. Luminescence was measured using the Cytation 3 plate reader (BioTek, Germany).

### 2.11. HPLC analysis of NCP metabolites

20–200 μM NCP was incubated with the cytosolic and microsomal fractions isolated from CCRF-CEM cells (3.5 mg of proteins per ml) and 0.5 mM GSH in 0.5 mM phosphate buffer pH 7.4 for 30 min at 37 °C. The reactions were stopped and extracted with methanol and chilled at −20 °C for 1 h. Then the samples were centrifuged at 8000 × *g* for 2 min in centrifugal filter units (Ultrafree-MC dura 0.22 μm, Millipore). The filtrates (50 μl) were injected onto the Supelcosil LC-18-S HPLC column (150 mm × 4.6 mm I. D., 5 μm). Mobile phase A corresponded to 50 mM phosphate buffer (PB) with 30% acetonitrile (v/v), mobile phase B to 50 mM PB with 10% acetonitrile (v/v) and mobile phase C to 50 mM PB. The gradient started with 100% mobile phase C going isocratically in 5 min, followed by steep change from C to B in 6 min, ongoing nonlinearly to 50% B in 20 min and then going linearly to 100% mobile phase A in 35 min. The flow rate was 0.9 ml $min^{-1}$. The absorption spectra of the eluate were recorded by a PDA detector. The data were analyzed at 260 nm.

### 2.12. GST and LO activity assays

2 μl of 0.1 M GSH were mixed with 10 μl of cytosolic or microsomal fraction (3.5 mg of proteins per ml) and 186 μl of phosphate buffer (0.1 M, pH=6.5) in 96-well plate. The reaction was started by the addition of 2 μl of 0.1 M CDNB. The GST-catalyzed formation of GS-DNB was detected immediately at 340 nm every minute for 15 min. LO activity was analyzed by Lipoxygenase Inhibitor Screening Assay Kit (Abnova, Walnut, CA, USA) according to the manufacturer's instructions. The reaction was initiated by adding 5 μl of substrate (linoleic acid) to 50 μl of CCRF-CEM crude extract (2.3 mg of proteins per ml) or 50 μl 15-lipoxygenase standard solution (100% initial activity) and incubated for 10 min. The enzyme catalysis was stopped by 50 μl of chromogen and the absorbance was readied after 5 min at 490 nm.

### 2.13. Cytotoxicity evaluation

The cytotoxicity of the tested compounds was assessed with use of XTT cell proliferation kit II (Roche Diagnostics GmbH, Mannheim, Germany) according to the manufacturer's instructions. Briefly CCRF-CEM and BGM cells were seeded in a 96-well plate at a density of 13,500 and 4000 cells per well, respectively. After 24 h, the tested compounds were added to the culture media and incubated for 72 h before the XTT dye was added. The absorbance at 495 nm was recorded after 1 h incubation with the dye. $IC_{50}$ values were determined by GraphPad Prism version 5.00 for Windows (GraphPad Software, La Jolla, CA, USA). Where indicated, cells were preincubated with 50 μM BSO (GSH biosynthesis inhibitor) for 24 h prior to the addition of NCP.

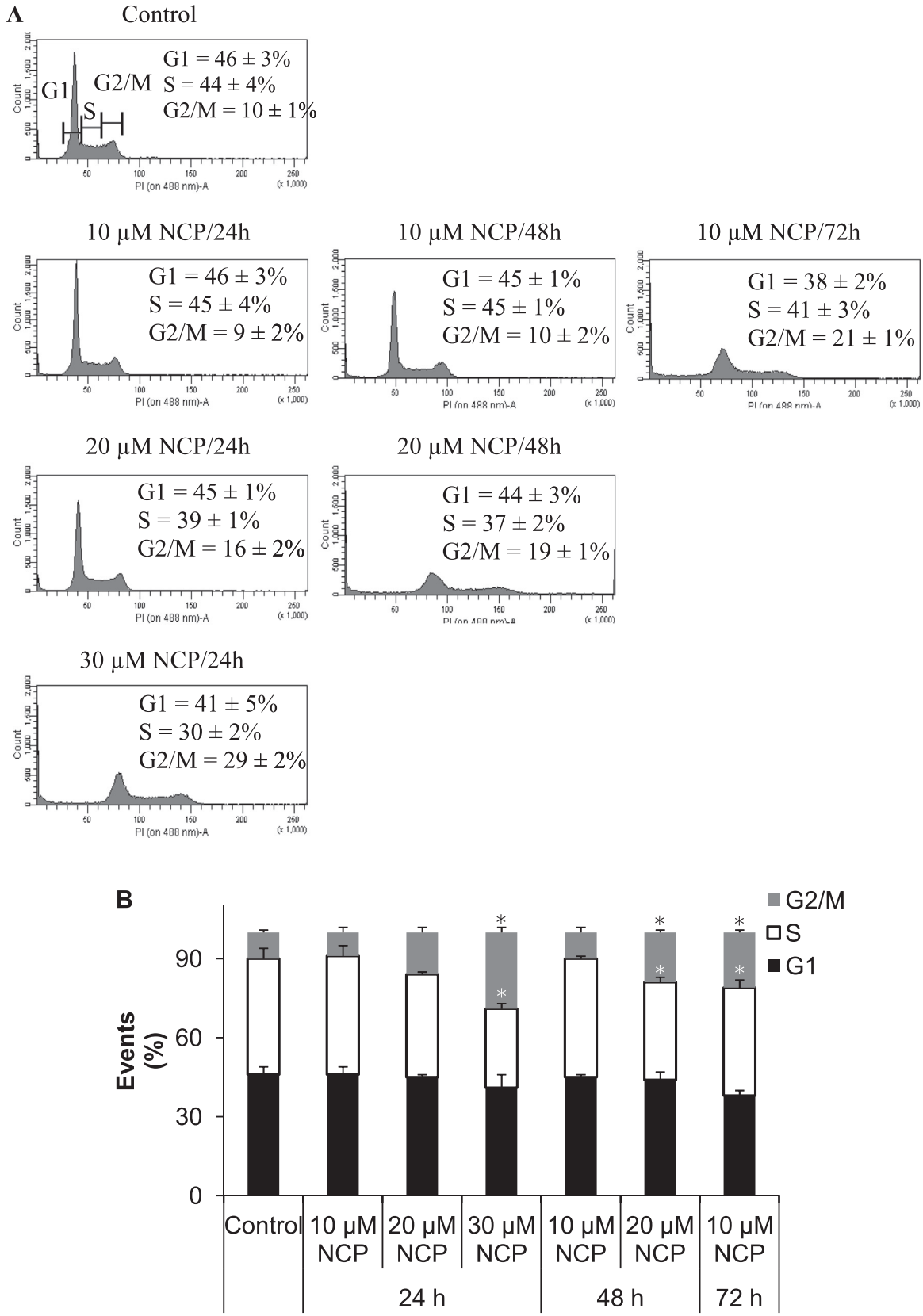


**Fig. 2.** NCP effect on cell cycle in CCRF-CEM cells. Cells were incubated with 10–30 μM NCP for 24–72 h. The DNA content was measured by flow cytometry and the percentage of cell cycle distribution was analyzed by ModFit software. The data for 72 h incubation with 20 μM NCP and 48 h and 72 h incubation with 30 μM NCP are not available due to extensive DNA fragmentation accompanying cell death. Representative histograms are shown in (A). The proportion of the cells in G1, S and G2/M phase together with the statistical evaluation is depicted in (B). Data represent the means ± SD, n = 3. *$P < 0.05$ vs. untreated control (ANOVA).

### 2.14. Statistical evaluation

Unless otherwise indicated, the data are presented as means ± SD from at least 3 independent experiments. The differences between the individual treatments were analyzed by ANOVA with Dunnett's post-hoc test (GraphPad Prism La Jolla, CA USA).

## 3. Results

### 3.1. NCP triggers cell cycle arrest and apoptosis

Previous findings indicated a selective effect of NCP on cell viability depending on the cell type [7]. In order to establish whether the observed cytotoxicity was accompanied by a disruption of cell cycle and/or apoptosis induction, CCRF-CEM cells were treated with 10–30 μM NCP –the concentrations near its $IC_{50}$ from the cytotoxicity assay (18.0 ± 1.8 μM). DNA contents analysis revealed that NCP induced cell cycle arrest in G2/M phase. The proportion of the cells in G2/M phase increased 2 to 3-fold compared to untreated control depending on the incubation conditions (Fig. 2).

NCP also significantly increased the percentage of Annexin V-positive cells compared to untreated control (Fig. 3A, B). Importantly, a distinct population of Annexin V-positive / PI-negative (i.e. "early apoptotic") cells was observed indicating a predominantly apoptotic mode of cell death. This is further supported by the activation of caspases (Fig. 3C). Although caspase activation followed a clear concentration-dependent pattern at both 4 and 24 h, Annexin V/PI assay was less sensitive at short incubation time (4 h) demonstrating a similar effect of 10–30 μM NCP. The results of both assays were comparable at 24 h incubation period. Pre-treatment of the cells with pan-caspase inhibitor Q-VD-OPh (10 μM) decreased the percentage of total Annexin V-positive cells from 35% to 23% indicating that caspases are at least partially involved in NCP-induced cell death (Fig. 4). Given the previously identified GSH reactivity with NCP [7], a possible role of GSH depletion in NCP-induced apoptosis was investigated. Therefore, cells were pre-incubated with GSH (3 mM) or *N*-acetylcysteine (3 mM) prior to the addition of 20 μM NCP. Indeed, following the 24 h of incubation, the percentage of the apoptotic cells in pre-treated samples decreased by 30% compared to the samples treated with NCP only, i.e. to the level of untreated control or even slightly below that level (Fig. 4).

### 3.2. NCP induces rapid GSH depletion accompanied by ROS production and lipid peroxidation

A major effect of the antioxidants on the extent of the apoptosis observed in NCP-treated CCRF-CEM cells led us to an investigation of their oxidative status. It was found, that GSH level in NCP-treated cells dropped to 3–65% of untreated control as early as after 2–4 h of incubation depending on the concentration used. At

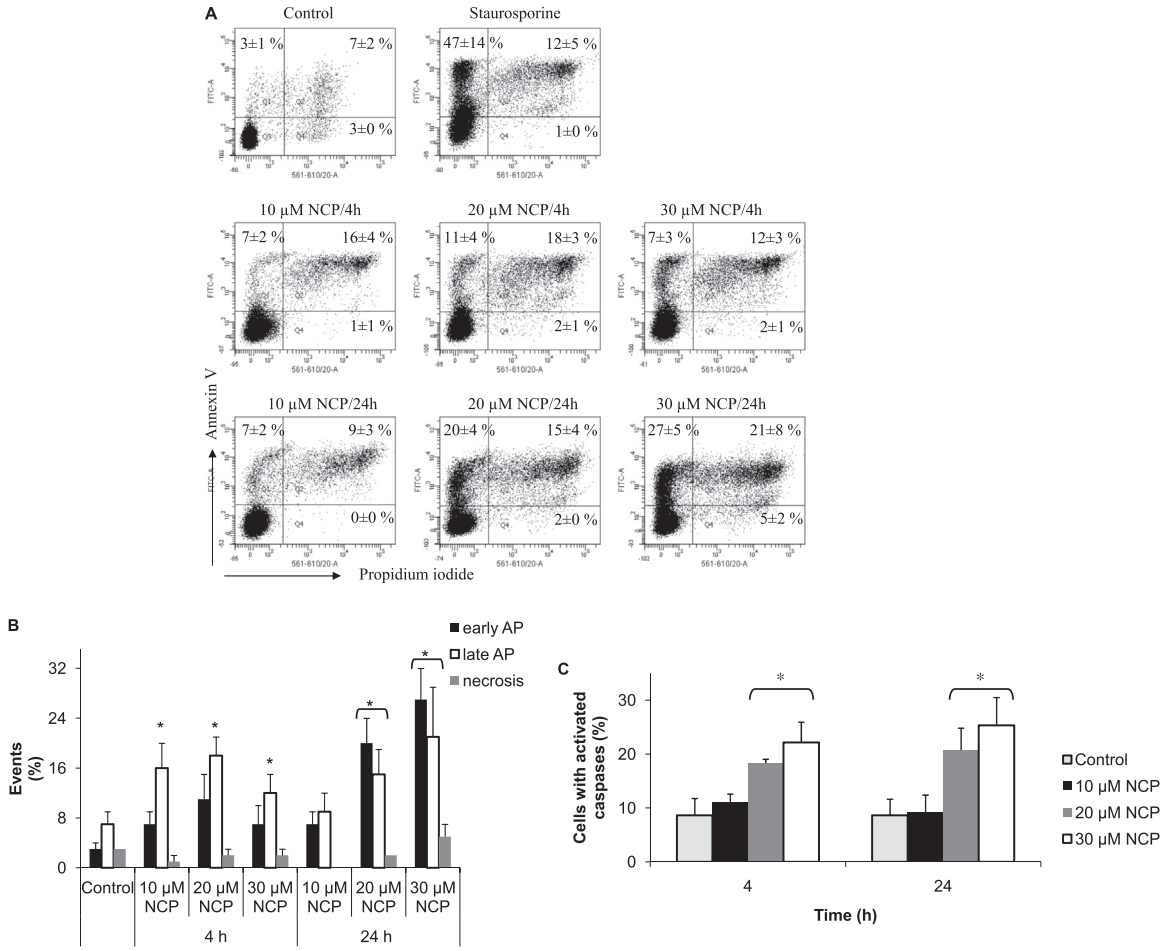


**Fig. 3.** NCP effect on apoptosis (AP) in CCRF-CEM cells. Cells were incubated with the indicated concentration of NCP for 4 or 24 h. 1 μM staurosporine was used as positive control. The extent of apoptosis was evaluated using the Dead Cell Apoptosis Kit with Annexin V Alexa Fluor® 488 & Propidium Iodide (A, B) or CaspACE™ FITC-VAD-FMK In Situ Marker (C). Representative dot plots are shown in (A). Upper-left quadrant: early (AP); upper-right: late AP/necrosis; lower-left: viable cells; lower-right: necrosis. The percentage of early and late apoptotic and necrotic cells together with the statistical evaluation is showed in (B). Data represent the means ± SD, n = 3. *P < 0.05 vs. untreated control (ANOVA).

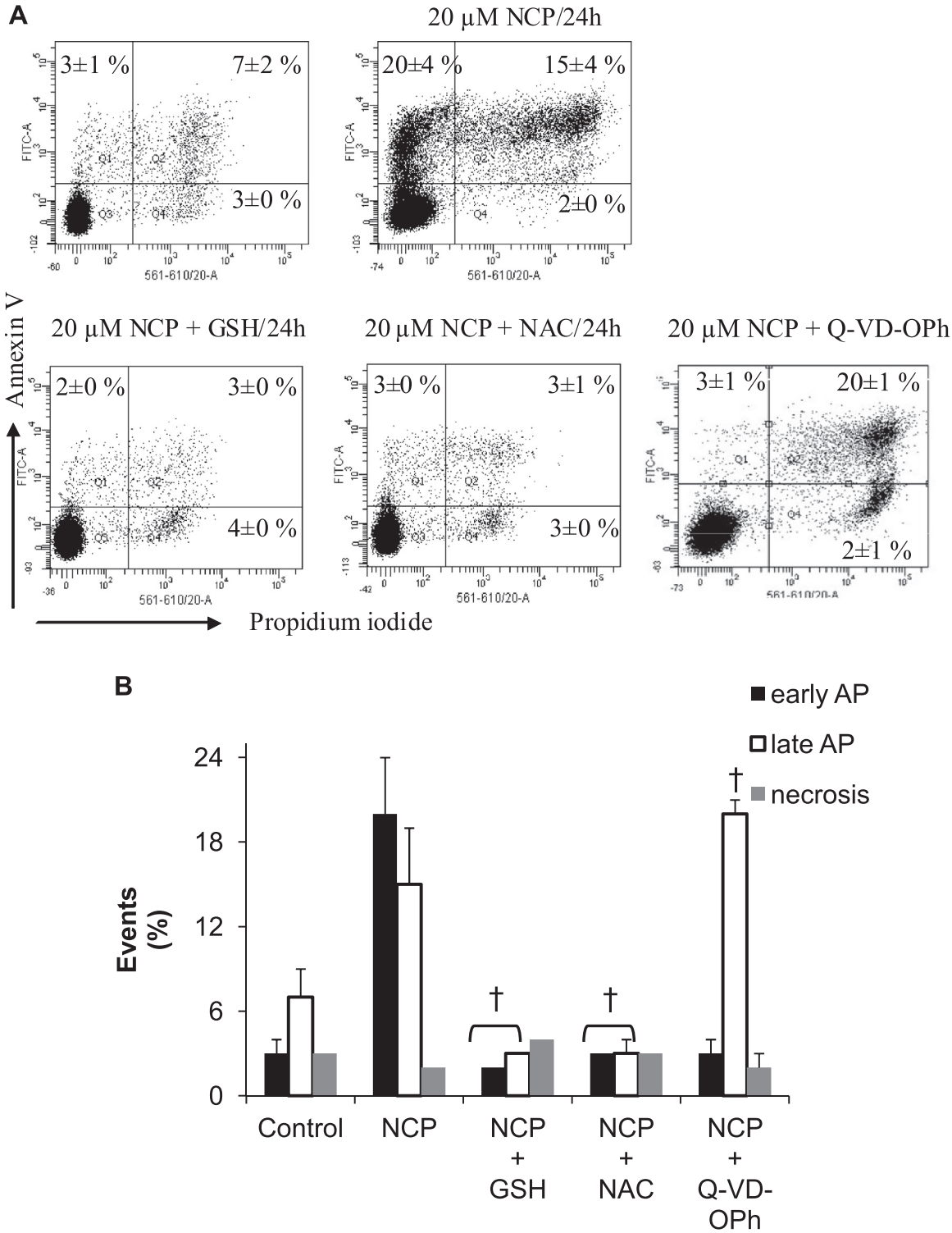


**Fig. 4.** The effect of thiols and caspase inhibition on NCP-induced apoptosis in CCRF-CEM cells. Cells pre-treated with GSH, NAC (both 3 mM) or pan-caspase inhibitor Q-VD-OPh (10 μM) for 0.5 h were incubated with 20 μM NCP for 24 h. Dual annexin V/PI staining was used as in Fig. 3 to quantify the extent of apoptosis. Representative dot plots are shown in (A). Upper-left quadrant: early (AP); upper-right: late AP/necrosis; lower-left: viable cells; lower-right: necrosis. Percentage of early and late apoptotic and necrotic cells together with the statistical evaluation is showed in (B). Data represent the means ± SD, n = 3. †$P < 0.05$ vs. NCP (ANOVA).

24 h the GSH level was back to the basal concentration or even higher within the whole concentration range (Fig. 5A).

ROS level in NCP-treated cells followed a similar, only slightly delayed pattern. ROS increase was detected already at 2 h of incubation (9 to 14-fold), maximal values were reached at 4 h (260 to 500-fold) and dropped again near baseline at 24 h (Fig. 5B). Accordingly, lipid peroxidation (measured as malondialdehyde level) in NCP-treated cells was also on the highest increase after 4 h of incubation with NCP (Fig. 5D). Interestingly, NCP also slightly but significantly increased lipoxygenase activity (Fig. 5E).

Subsequently, the origin of ROS was investigated using various inhibitors of ROS generation: CCCP (10 μM), DPI (10 μM), ABT (0.25 mM), ALLO (0.5 mM), CAPE (10 μM) and 4-PBA (5 mM). The antioxidants GSH (3 mM), NAC (3 mM) and QUER (10 μM) were

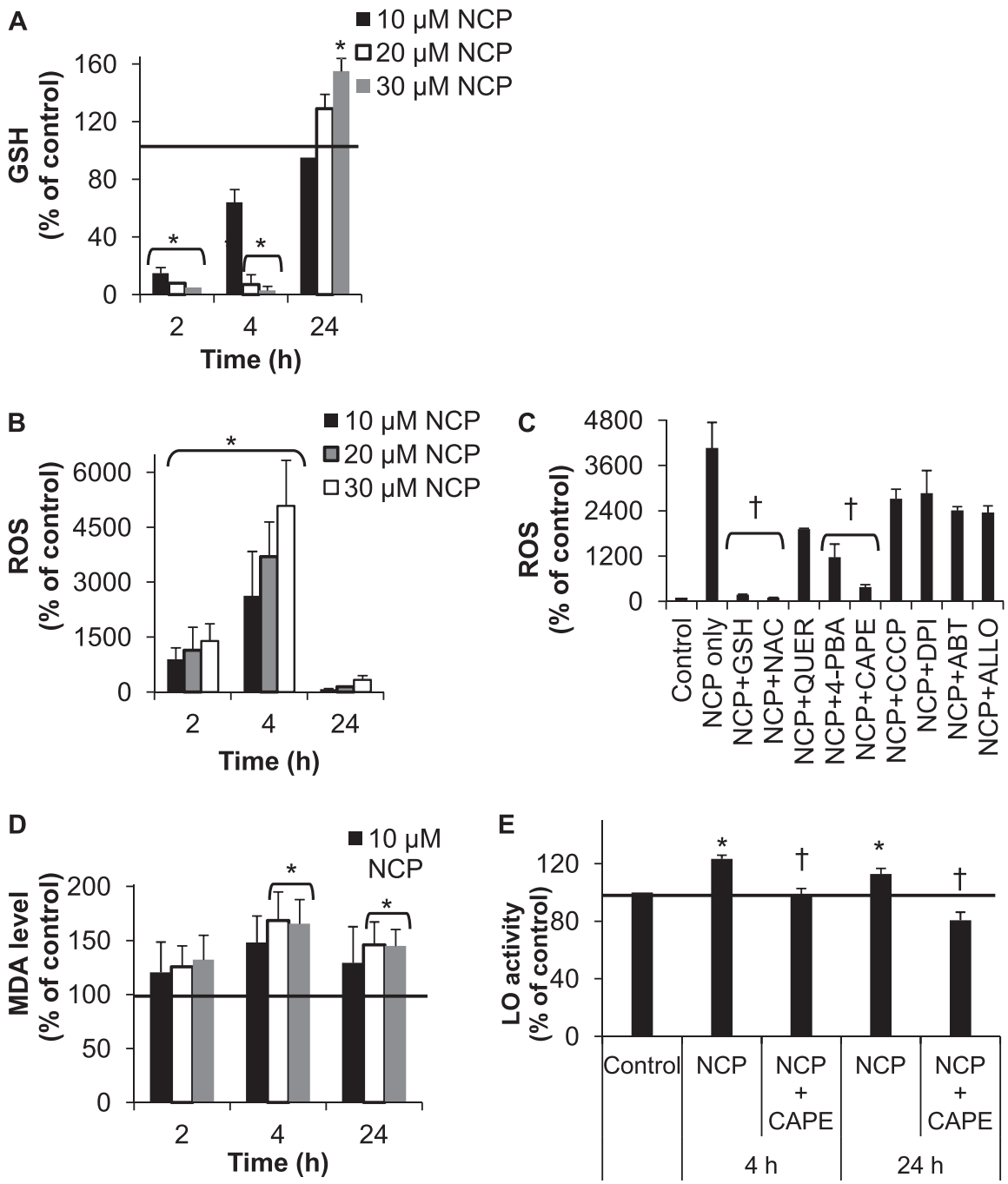


**Fig. 5.** NCP effect on the oxidative status of CCRF-CEM cells. Cells were incubated with the indicated concentration of NCP for 2–24 h (A, B, D) or alternatively, pre-treated with specific antioxidants/inhibitors for 0.5 h prior to the addition of 20 μM NCP (C,E). GSH level in NCP-treated cells is expressed as the percentage of untreated control ($2.4 \pm 0.2$ μM GSH/$10^6$ cells, A). ROS level in NCP-treated cells is expressed as the percentage of DCF fluorescence intensity in untreated sample (B). The effect of inhibitors of various metabolic pathways and antioxidants on NCP-induced ROS production (C). The effect of NCP on lipid peroxidation is expressed as the percentage of MDA in untreated control ($1.0 \pm 0.1$ μM/$10^6$ cells, D). Lipoxygenase (LO) activity in NCP-treated cells is expressed as the percentage of untreated control (E). All data represent the means ± SD, n = 3. *$P < 0.05$ vs. untreated control. †$P < 0.05$ vs. NCP only (ANOVA).

also employed. Significant, though not complete, inhibition of ROS production was detected in the cells pre-treated with 4-PBA and CAPE (Fig. 5C). An absolute reversion of ROS production was only observed with the antioxidants. QUER, a free radical scavenger, was significantly less effective compared to the thiols (GSH, NAC). This all suggests the provenance of ROS from multiple sources with sulfhydryl depletion playing a major, initiating role while lipid peroxidation and ER stress are involved in further ROS promotion.

### 3.3. NCP activates Nrf2 pathway

Many recent reports demonstrate that glutathione depletion activates Nrf2 pathway. An immunoblotting analysis of the nuclear fraction of NCP-treated CCRF-CEM cells was performed to assess a subcellular distribution of Nrf2. We found a rapid (0.5–1 h) translocation of Nrf2 to the nuclei in response to NCP treatment (Fig. 6A). Further, we investigated two Nrf2 downstream targets, NQO-1 and GCLm. Following the 24 h treatment of the cells with NCP, both

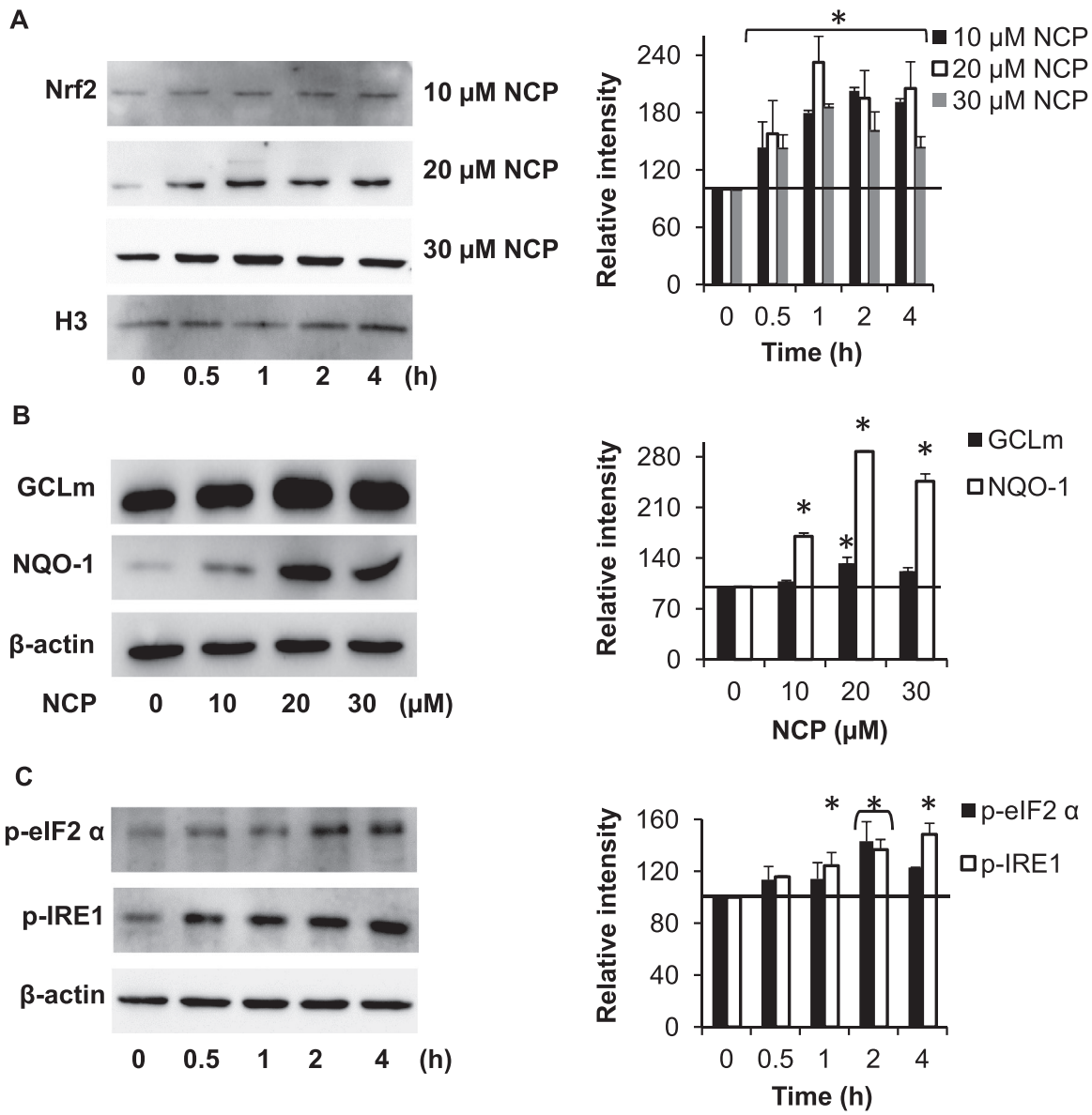


**Fig. 6.** Activation of Nrf2- and ER stress-related pathways by NCP. Cells were incubated with the indicated concentration of NCP. After the incubation, nuclear fraction (A, 0–4 h incubation), whole cell lysate (B, 24 h incubation) or membrane proteins (C, 0–4 h incubation) were resolved by SDS-PAGE and probed with specific antibodies. Densitometric analysis is shown to the right of each Western blot. Results were normalized by arbitrarily setting the density of untreated cells to 100%. Data represent the means ± SD, n = 3. *P < 0.05 vs. untreated control (ANOVA).

proteins were overexpressed in a concentration-dependent manner (Fig. 6B).

### 3.4. NCP induces ER stress, mitochondrial depolarization and ATP decrease

The role of ER stress in NCP-induced apoptosis was studied by monitoring the activation of two major ER-stress related pathways, i.e. eIE2α and IRE1. The results showed that NCP (20 μM) induced an early increase in the phosphorylation of both proteins (Fig. 6C) suggesting the presence of ER stress.

With respect to the known fact that NCP undergoes GST-catalyzed conjugation with the GSH, we have determined the contribution of the microsomal and the cytosolic GSTs aiming to evaluate the role of local GSH decrease directly in the ER to the development of ER stress. To this end, subcellular fractions isolated from untreated CCRF-CEM cells were employed. Following the incubation of the respective fractions with 20–200 μM NCP and 0.5 mM GSH for 30 min, we found 100% conversion in the cytosol vs. no conversion in the microsomes. To avoid false negative results the GST activity in both fractions was measured using CDNB as a substrate and was found to be 558 ± 113 ncat/mg in the cytosol and 72 ± 27 ncat/mg in the microsomes.

To further examine whether the NCP-induced oxidative and ER stress also affects mitochondria, MMP was determined. It was found that NCP caused a time- and concentration-dependent MMP loss (Fig. 7A). The pre-treatment of the cells with 5 mM 4-PBA (an ER stress inhibitor) abolished this effect at 4 h but not at 24 h because of its inherent cytotoxic effect at longer incubation times (data not shown). On the other hand, the pre-treatment of the cells with antioxidants, GSH (3 mM) and NAC (3 mM), prevented the MMP loss for up to 24 h incubation (Fig. 7B).

The ATP level following the 2–24 h of NCP treatment corresponded well with mitochondria condition. Intracellular ATP concentrations decreased for up to 25% compared to untreated control (Fig. 7C). The effect of NCP on mitochondrial ROS was also

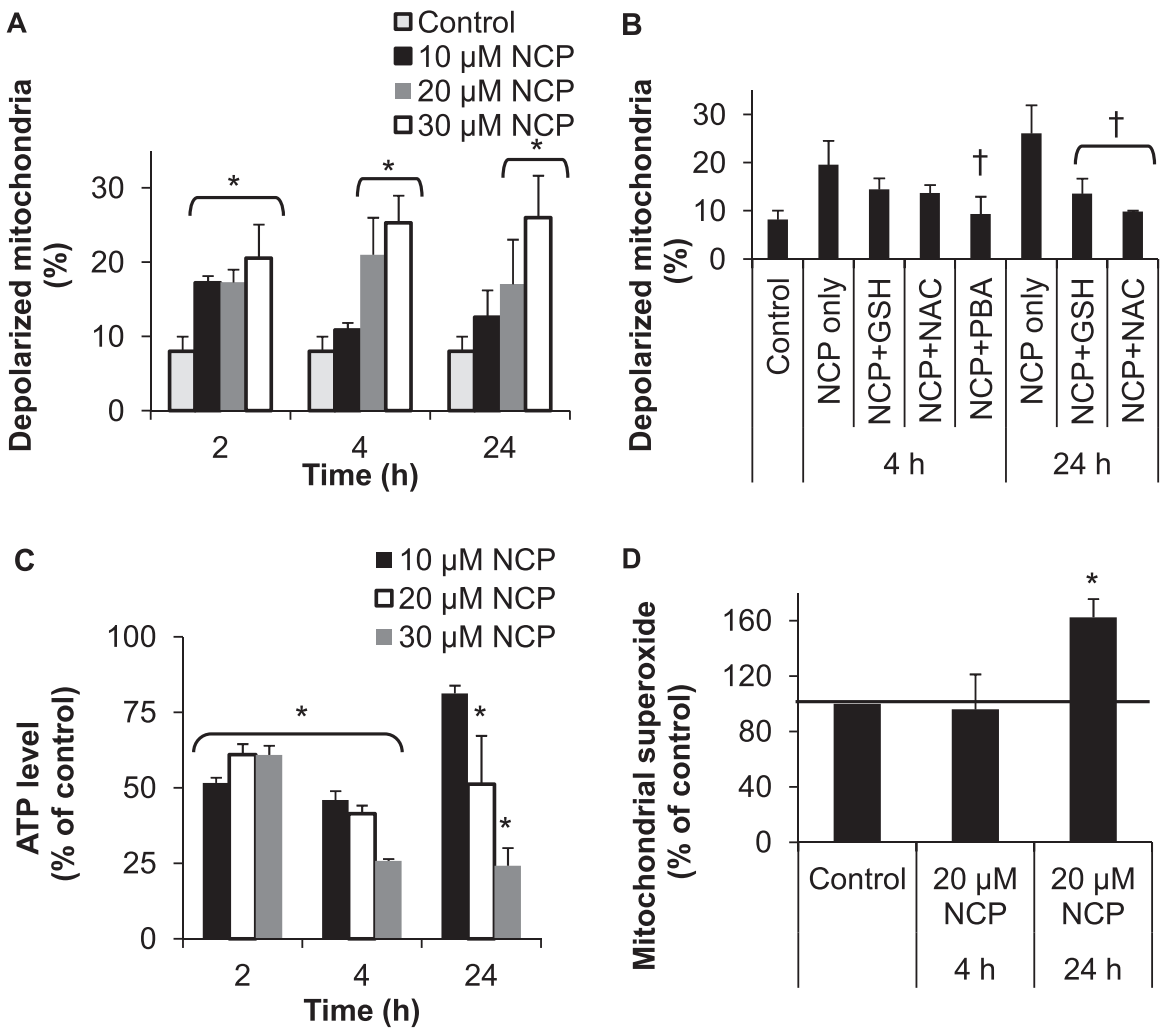


**Fig. 7.** NCP effect on mitochondrial function in CCRF-CEM cells. Cells were incubated with the indicated concentration of NCP for 2–24 h (A,C,D) or pre-treated with specific inhibitors for 0.5 h prior to the addition of 20 μM NCP for 4 h (B). Mitochondrial membrane potential (MMP) was determined with the use of JC-1 probe and flow cytometric detection. The data are presented as the percentage of de-energized mitochondria (A, B). The ATP level in NCP-treated cells was quantified by CellTiter-Glo® assay (C). The absolute value of ATP in untreated sample = 4.2 ± 0.1 mM. Mitochondrial superoxides were detected with the use of MitoSOX™ probe and quantified by flow cytometry (D). The data are expressed as the percentage of untreated control (100%) and represent means ± SD, n = 3. *P < 0.05 vs. untreated control. †P < 0.05 vs. NCP only (ANOVA).

**Table 1**
Effect of chloropurine-caused GSH depletion on cytotoxicity in CCRF-CEM and BGM cells.

| Comp. | CCRF-CEM | | | | BGM | | |
|---|---|---|---|---|---|---|---|
| | GSH decrease (%)[a] | GSH decrease $EC_{50}$ (μM)[b] | Cell viability (%)[c] | Cell viability $IC_{50}$ (μM)[d] | GSH decrease (%)[a] | Cell viability (%)[c] | Cell viability $IC_{50}$ (μM)[d] |
| **1** (NCP) | 8 ± 3 | 4.5 ± 0.1 | 16 ± 8 | 18.0 ± 1.8 | 62 ± 17 | 111 ± 6 | ≥ 50 |
| **2** | 12 ± 3 | 4.9 ± 0.1 | 35 ± 10 | 23.3 ± 1.6 | 57 ± 10 | 96 ± 18 | ≥ 50 |
| **3** | 11 ± 3 | 6.8 ± 1.6 | 50 ± 11 | 22.1 ± 0.7 | 58 ± 14 | 104 ± 10 | ≥ 50 |
| **4** | 7 ± 3 | 2.7 ± 0.1 | 9 ± 1 | 7.6 ± 0.4 | 60 ± 11 | 106 ± 6 | ≥ 50 |
| **5** | 1 ± 0 | 4.9 ± 1.3 | 15 ± 6 | 16.6 ± 2.2 | 61 ± 18 | 104 ± 11 | ≥ 50 |
| **6** | 4 ± 2 | 3.2 ± 0.1 | 11 ± 4 | 7.9 ± 0.4 | 54 ± 7 | 109 ± 10 | ≥ 50 |
| **7** | 3 ± 1 | 4.5 ± 0.5 | 8 ± 1 | 11.1 ± 0.8 | 70 ± 11 | 101 ± 5 | ≥ 50 |
| **8** | 76 ± 3 | NA | 107 ± 8 | ≥ 50 | 73 ± 11 | 116 ± 4 | ≥ 50 |
| **9** | 75 ± 8 | NA | 91 ± 11 | ≥ 50 | 82 ± 14 | 98 ± 5 | ≥ 50 |

Data are means ± SD from three independent experiments. Control (BGM) = 6.5 ± 0.8 μM GSH/$10^6$ cells. Control (CCRF-CEM) = 2.4 ± 0.2 μM GSH/$10^6$ cells.

[a] 4 h treatment with 20 μM compounds; untreated control = 100% GSH.

[b] $EC_{50}$ value indicates the concentration of a compound causing 50% decrease in cellular GSH content after 4 h incubation (calculated using the non-linear regression method by GraphPad Prism).

[c] 72 h treatment with 20 μM compounds; untreated control = 100% viability.

[d] $IC_{50}$ value indicates the concentration of a compound causing 50% decrease in cells viability in XTT assay after 72 h incubation (calculated using the non-linear regression method by GraphPad Prism).

investigated. The mitochondrial superoxides were increased for up to 1.5-fold after 24 h (but not 4 h) incubation with 20 μM NCP indicating the (secondary) mitochondrial damage (Fig. 7D).

### 3.5. Cytotoxicity of 9-norbornyl-6-chloropurine derivatives correlates with their GSH-depleting potency

To provide evidence that the observed cellular effects of NCP ultimately leading to the apoptotic cell death are indeed GSH-dependent, we assayed a series of 8 additional 9-norbornylpurine derivatives (Fig. 1) for their cytotoxicity and the effect on GSH level in both leukemia (CCRF-CEM) and normal epithelial (BGM) cells. It was found, that GSH level in treated cells dropped to 1–76% of untreated control in CCRF-CEM cells after 4 h of incubation. Importantly, the derivatives lacking the GSH-lowering capacity were also the least cytotoxic of the group (Table 1). Interestingly, both inactive derivatives (**8** and **9**) are substituted at the position 8. Other modifications (on both norbornane moiety or purine ring) apparently did not make a significant impact on the biological activity. Compounds **2–7** were all capable of a marked and rapid depletion of GSH pool and were also cytotoxic in CCRF-CEM cells. However, $EC_{50}$ titration for GSH-lowering capacity revealed subtle differences among the compounds, which largely correlate with their cytotoxic $IC_{50}$.

The decrease of GSH level in BGM cells ranged between 54% and 82% (Table 1). No cytotoxicity was observed, when BGM cells were treated with 20 μM compounds. Their $IC_{50}$ for a cytotoxic effect exceeded the maximal tested concentration of compounds (50 μM) (Table 1).

## 4. Discussion

9-Norbornyl-6-chloropurines (Fig. 1) are a novel class of antiviral and cytotoxic compounds. NCP, a representative structure within this class, has been previously identified as a promising antileukemic agent because of its highly selective cytotoxicity towards leukemia cell lines ($IC_{50}$ ~20 μM) vs. solid tumor cell lines ($IC_{50}$ ~150 μM) or noncancerous cells ($IC_{50}$ ~500 μM) [7]. We here provide evidence that the compound induces apoptotic cell death through NCP-triggered GSH depletion.

As described previously, NCP was shown to be a substrate for GST, forming a GSH conjugate (NCP-GS) as a major metabolite that is excreted from the cells [7]. Reduced GSH is the most abundant low molecular weight thiol in animal cells and is involved in many cellular processes [26]. Also, GSH is the main redox buffer in the cells and GSH/GSSG ratio is an accepted indicator of intracellular redox status [27]. We found that GSH level was rapidly decreased in NCP-treated cells, but it was also quickly replenished by 24 h of incubation (Fig. 5A). As expected, ROS level followed a complementary pattern i.e. an initial increase that was followed by a drop near baseline (Fig. 5B). MDA levels remained elevated at 24 h, which is not particularly surprising since it is a relatively stable oxidation product with considerably higher half-life compared to ROS. A fast cellular response to NCP-induced oxidative stress suggested an activation of antioxidant defense system [28,29]. Indeed, we have observed a rapid activation of Nrf2 pathway as documented by phosphorylation and a translocation of Nrf2 to nuclei (Fig. 6A). This was associated with an induction of Nrf2 downstream targets, such as NQO-1 and GCLm (Fig. 6B). The latter directly explains the observed restoration of GSH level to basal conditions or even higher than that. Despite the early activation of the antioxidant signalling, NCP still triggered apoptosis in CCRF-CEM cells (Fig. 3). The induction of cell death by NCP may indicate that the repair mechanisms have been overwhelmed by the critical amount of ROS as previously suggested by others [30,31]. The fact that the GSH- or NAC-pretreated cells remained resistant to the cytotoxic/apoptotic effects of NCP (Fig. 4) points to an essential role of GSH in the apoptotic signalling induced by NCP.

ROS have been known to activate ER apoptotic death pathways [32] and ER-associated stress allows ROS to be generated by the mitochondria contributing to mitochondria-associated cell death [33]. Also, mitochondria-associated ROS in return may enhance ER stress response [34]. A number of compounds have been reported to induce apoptosis in various cells through both ER and mitochondrial pathways, e.g. curcumin or furanodien [35,36]. We have shown that NCP affects mitochondria by inducing MMP loss, ATP production decrease and mitochondrial superoxide generation (Fig. 7A, C, D). We also demonstrated that NCP induced PERK/eIF2α and IRE1 phosphorylation clearly indicating the activation of at least two pathways of the unfolded protein response (Fig. 6C). Moreover, the inhibition of ER stress by 4-PBA reversed mitochondrial depolarization induced by NCP. Similar effect was observed with the antioxidants NAC and GSH, again pointing to a key role of GSH level in NCP-induced cellular effects (Fig. 7B). In addition, 4-PBA was also effective in inhibiting NCP-induced ROS generation surpassing the effect of quercetin, the known inhibitor of lipid peroxidation and potent antioxidant. However, quercetin also reacts with cellular thiols [37], which may explain its weak protection against NCP-induced ROS production. Notably, NCP was not a substrate for the microsomal GSTs suggesting that the presumed loss of local (microsomal) GSH is not the direct trigger for ER stress development.

Interestingly, lipoxygenase (LO) inhibitor CAPE was found to be very effective in ROS inhibition (Fig. 5C). 5-LO was indeed slightly activated by the action of NCP and CAPE prevented this effect, however, it seems unlikely that this would be the major factor determining such a huge protectivity against NCP-induced ROS increase. In fact, the effects of CAPE on the cells are rather pleiotropic. In addition to LO inhibition, it is also a known radical scavenger and a compound with anti-inflammatory effects [38,39]. Therefore, several events could contribute to its overall protective effect. GSH redox system and mitochondrial dysfunction have crucial role in the regulation of cell cycle as well [40–42]. NCP was found to cause concentration- and time-dependent cell cycle arrest in G2/M phase, which is apparently tightly connected with the apoptotic potency of NCP (Fig. 2). G2/M phase arrest has also been reported in several cell lines for another GSH-reactive anticancer compound – sulphoraphane [43]. NCP-induced cell death has been shown to be caspase-mediated, although other mechanisms seem to be also involved. The apparent inconsistency of the data pointing to the actual increase in late apoptotic population following the caspase inhibition, can be explained by the fact that using the Annexin V/PI assay it is not possible to distinguish between late apoptotic and necrotic cells. It is therefore likely that the inhibition of caspases drives NCP-induced cell death towards necrosis rather than apoptosis.

To date, a combination chemotherapy rather than a single agent treatment is the standard in clinical practice. Whereas elevated GSH levels are associated with tumor cell resistance [44], depletion of intracellular GSH has been recognized to result in enhanced toxicity of various chemotherapeutic agents in drug-resistant tumors. For example, N-methylformamide improved the response of colon cancer cells to doxorubicin and cisplatin [45]. Also, pre-treatment of the antihormone-resistant breast cancer cells with buthionine sulfoximine was found to increase their sensitivity to estradiol-induced apoptosis [46]. The capacity of NCP to decrease GSH level, induce ROS overproduction, ER stress and mitochondrial dysfunction may therefore be especially advantageous in various combination regimens. On the other hand, sustained low doses of NCP that do not induce apoptosis could be eventually chemoprotective due to its ability to induce Nrf2 pathway and boost cellular antioxidant defense. Also in this respect, NCP appears to resemble the natural

isothiocyanate sulphoraphane. This particular property of NCP may also be responsible for its relatively high (micromolar) $IC_{50}$ in the cytotoxicity assay.

To address the question whether the cytotoxicity correlated with GSH levels in treated cells, a panel of variously substituted 9-norbornyl-6-chloropurines was employed (Fig. 1). Apart from leukemia CCRF-CEM cells, BGM kidney epithelial cells, commonly used for antiviral screening, were included to this experiment. Using these cells, connection between the depletion of intracellular GSH and defective virion morphogenesis of enteroviruses has been previously demonstrated [47]. All compounds used in this study except for 8-substituted compounds (**8** and **9**) lowered cellular GSH with similar (good) efficiency (Table 1). Obviously, substitution at the position 8 completely abolished both cytotoxicity and the capacity of the compounds to modulate GSH level in the cells. This is likely due to the impaired interaction of these compounds with GST - we found that non-enzymatic conjugation of NCP with the GSH was negligible [7]. The drop in GSH level caused by 9-norbornyl-6-chloropurines was smaller in BGM than that in CCRF-CEM cells (Table 1) and the viability of BGM cells remained unaffected. These results can be explained by a different basal level of GSH in these two cell lines, which was almost three times higher in BGM than in CCRF-CEM cells. Although we can expect equivalent loss of GSH in both CCRF-CEM and BGM cells due to its interaction with the same amount of the inhibitor (20 μM), the levels of remaining GSH will be different. Whilst this residual GSH does not cover the needs of the CCRF-CEM cells, in case of BGM cells it is still sufficient to protect them from oxidative stress. Moreover, cytotoxic effect of 9-norbornyl-6-chloropurines in CCRF-CEM cells can be pronounced by a very low activity of catalase in this cell line [48]. Therefore, we can conclude that the ability of norbornylpurines to lower GSH is critical for inducing cell death. Interestingly, various substitutions on the norbornane moiety did not make remarkable difference in compounds ability to influence cell viability or GSH level. Subtle differences observed among the series more likely result from their distinct physico-chemical properties e.g. lipophilicity, thus affecting membrane permeability and cellular uptake.

In summary, we described the key role of GSH depletion in NCP-induced cell death through ER stress activation and mitochondrial dysfunction. Furthermore, NCP was found to overcome cellular defense mechanisms at longer incubation times or high concentrations used and thus inducing G2/M arrest and apoptosis. Our data suggest the potential of NCP as a novel antileukemic drug, especially in combination chemotherapy and provides important information regarding the development of a GSH-depleting strategy.

## Conflict of interest

None.

## Acknowledgments

The study was supported by the project InterBioMed #LO1302 from the Ministry of Education of the Czech Republic, the Grant Agency of the Czech Republic #P303/11/1297 and the Research Project of the IOCB #RVO:61388963.

## References

[1] M. Šála, H. Hřebabecký, P. Leyssen, M. Dejmek, M. Dračínský, A.M. De Palma, J. Neyts, R. Nencka, Novel substituted 9-norbornylpurines and their activities against RNA viruses, Bioorg. Med. Chem. Lett. 22 (2012) 1963–1968.
[2] M. Dejmek, M. Šála, P. Plačková, H. Hřebabecký, L. Borreda, M.J. Neyts, M. Dračínský, E. Procházková, P. Jansa, P. Leyssen, H. Mertlíková-Kaiserová, R. Nencka, Synthesis of novel purine-based coxsackievirus inhibitors bearing polycylic substituents at the N-9 position, Arch. Pharm. 347 (2014) 478–485.
[3] H. Hřebabecký, M. Dejmek, M. Šála, H. Mertlíková-Kaiserová, M. Dračínský, P. Leyssen, J. Neyts, R. Nencka, Synthesis of novel thienonorbornylpurine derivatives, Tetrahedron 68 (2012) 3195–3204.
[4] H. Hřebabecký, M. Dejmek, M. Dračínský, M. Šála, P. Leyssen, J. Neyts, M. Kaniaková, J. Krůšek, R. Nencka, Synthesis of novel azanorbornylpurine derivatives, Tetrahedron 68 (2012) 1286–1298.
[5] M. Šála, A.M. De Palma, H. Hřebabecký, M. Dejmek, M. Dračínský, P. Leyssen, J. Neyts, H. Mertlíková-Kaiserová, R. Nencka, SAR studies of 9-norbornylpurines as Coxsackievirus B3 inhibitors, Bioorg. Med. Chem. Lett. 21 (2011) 4271–4275.
[6] P. Plačková, H. Hřebabecký, M. Šála, R. Nencka, T. Elbert, H. Mertlíková-Kaiserová, Transport mechanisms of a novel antileukemic and antiviral compound 9-norbornyl-6-chloropurine, J. Enzyme Inhib. Med. Chem. 30 (2015) 57–62.
[7] P. Plačková, N. Rozumová, H. Hřebabecký, M. Šála, R. Nencka, T. Elbert, A. Dvořáková, I. Votruba, H. Mertlíková-Kaiserová, 9-Norbornyl-6-chloropurine is a novel antileukemic compound interacting with cellular GSH, Anticancer Res. 33 (2013) 3163–3168.
[8] S. Toyokuni, K. Okamoto, J. Yodoi, H. Hiai, Persistent oxidative stress in cancer, FEBS Lett. 358 (1995) 1–3.
[9] A. Perjes, A.M. Kubin, A. Konyi, S. Szabados, A. Cziraki, R. Skoumal, H. Ruskoaho, I. Szokodi, Physiological regulation of cardiac contractility by endogenous reactive oxygen species, Acta Physiol. 205 (2012) 26–40.
[10] M. Halasi, M. Wang, T.S. Chavan, V. Gaponenko, N. Hay, A.L. Gartel, ROS inhibitor N-acetyl-L-cysteine antagonizes the activity of proteasome inhibitors, Biochem. J. 454 (2013) 201–208.
[11] J.D. Malhotra, R.J. Kaufman, Endoplasmic reticulum stress and oxidative stress: a vicious cycle or a double-edged sword? Antioxid. Redox Signal. 9 (2007) 2277–2293.
[12] V.I. Lushchak, Glutathione homeostasis and functions: potential targets for medical interventions, J. Amino Acids (2011) (2012), http://dx.doi.org/10.1155/2012/736837.
[13] J.S. Armstrong, K.K. Steinauer, B. Hornung, J.M. Irish, P. Lecane, G.W. Birrell, D. M. Peehl, S.J. Knox, Role of glutathione depletion and reactive oxygen species generation in apoptotic signaling in a human B lymphoma cell line, Cell Death Differ. 9 (2002) 252–263.
[14] M. Wang, R.J. Kaufman, The impact of the endoplasmic reticulum protein-folding environment on cancer development, Nat. Rev. Cancer 14 (2014) 581–597.
[15] D.G. Breckenridge, M. Germain, J.P. Mathai, M. Nguyen, G.C. Shore, Regulation of apoptosis by endoplasmic reticulum pathways, Oncogene 22 (2003) 8608–8618.
[16] A.Y. Choia, J.H. Choia, H. Yoona, K.Y. Hwanga, M.H. Noh, W. Choea, K.S. Yoona, J. Ha, E.J. Yeo, I. Kang, Luteolin induces apoptosis through endoplasmic reticulum stress and mitochondrial dysfunction in Neuro-2a mouse neuroblastoma cells. luteolin induces apoptosis, Eur. J. Pharmacol. 668 (2011) 115–126.
[17] T. Verfaillie, N. Rubio, A.D. Garg, G. Bultynck, R. Rizzuto, J.P. Decuypere, J. Piette, C. Linehan, S. Gupta, A. Samali, P. Agostinis, PERK is required at the ER-mitochondrial contact sites to convey apoptosis after ROS-based ER stress, Cell Death Differ. 19 (2012) 1880–1891.
[18] J. Henry-Mowatt, C. Dive, J.C. Martinou, D. James, Role of mitochondrial membrane permeabilization in apoptosis and cancer, Oncogene 23 (2004) 2850–2860.
[19] M. Loeffler, G. Kroemer, The mitochondrion in cell death control: certainties and incognita, Exp. Cell Res. 256 (2000) 19–26.
[20] J. Henry-Mowatt, C. Dive, J. Martinou, D. James, Mitochondria: in sickness and in health, Cell 148 (2012) 1145–1159.
[21] S.J. Ralph, P. Low, L. Dong, A. Lawen, J. Neuzil, Mitocans: mitochondrial targeted anti-cancer drugs as improved therapies and related patent documents, Recent Pat. Anticancer Drug Discov. 1 (2006) 327–346.
[22] H. Digaleh, M. Kiaei, F. Khodagholi, Nrf2 and Nrf1 signaling and ER stress crosstalk: implication for proteasomal degradation and autophagy, Cell Mol. Life Sci. 70 (2013) 4681–4694.
[23] T. Nguyen, P.J. Sherratt, C.B. Pickett, Regulatory mechanisms controlling gene expression mediated by the antioxidant response element, Annu. Rev. Pharmacol. Toxicol. 43 (2003) 233–260.
[24] M. Šála, A.M. De Palma, H. Hřebabecký, R. Nencka, M. Dračínský, P. Leyssen, J. Neyts, A. Holý, Design, synthesis, and biological evaluation of novel coxsackievirus B3 inhibitors, Bioorg. Med. Chem. 18 (2010) 4374–4384.
[25] I. Rahman, A. Kode, S.K. Biswas, Assay for quantitative determination of glutathione and glutathione disulfide levels using enzymatic recycling method, Nat. Protoc. 1 (2006) 3159–3165.
[26] R. Franco, M.I. Panayiotidis, J.A. Cidlowski, Glutathione depletion is necessary for apoptosis in lymphoid cells independent of reactive oxygen species formation, J. Biol. Chem. 42 (2007) 30452–30465.
[27] F.Q. Schafer, G.R. Buettner, Redox environment of the cell as viewed through the redox state of the glutathione disulfide/glutathione couple, Free Radic. Biol. Med. 30 (2001) 1191–1212.
[28] H. Li, S. Wu, J. Chen, B. Wang, N. Shi, Effect of glutathione depletion on Nrf2/ARE activation by deltamethrin in PC12 Cells, Arh. Hig. Rada Toksikol. 24 (2013) 87–97.
[29] K.W. Kang, S.J. Lee, S.G. Kim, Molecular mechanism of nrf2 activation by oxidative stress, Antioxid. Redox Signal. 7 (2005) 1664–1673.

[30] A.B. Granado-Serrano, M.A. Martín, L. Bravo, L. Goya, S. Ramos, Quercetin modulates Nrf2 and glutathione-related defenses in HepG2 cells: involvement of p38, Chem. Biol. Interact. 195 (2012) 154–164.
[31] C.E. Goldring, N.R. Kitteringham, R. Elsby, L.E. Randle, Y.N. Clement, D.P. Williams, M. McMahon, J.D. Hayes, K. Itoh, M. Yamamoto, B.K. Park, Activation of hepatic Nrf2 in vivo by acetaminophen in CD-1 mice, Hepatology 29 (2004) 1267–1276.
[32] J. Kim, M. Yun, E. Kim, D. Jung, G. Won, B. Kim, J.H. Jung, S. Kim, Generation of ROS by Decursin selectively induces the ER stress pathway components ATF4/PERK leading to the synergistic enhancement of TRAIL-induced apoptosis, Br. J. Pharmacol. (2015), http://dx.doi.org/10.1111/bph.13408.
[33] B. Bhandary, A. Marahatta, H.R. Kim, H.J. Chae, An involvement of oxidative stress in endoplasmic reticulum stress and its associated diseases, Int. J. Mol. Sci. 14 (2012) 434–456.
[34] Y. Hyonok, K. Do-Sung, L. Geum-Hwa, K. Kee-Won, K. Hyung-Ryong, Ch Han-Jung, Apoptosis induced by manganese on neuronal SK-N-MC cell line: endoplasmic reticulum (ER) stress and mitochondria dysfunction, Environ. Health Toxicol. 26 (2011) e2011017.
[35] S.H. Wu, L.W. Hang, J.S. Yang, H.Y. Chen, H.Y. Lin, J.H. Chiang, C.C. Lu, J.L. Yang, T.Y. Lai, Y.C. Ko, J.G. Chung, Curcumin induces apoptosis in human non-small cell lung cancer NCI-H460 cells through ER stress and caspase cascade- and mitochondria-dependent pathways, Anticancer Res. 30 (2010) 2125–2133.
[36] W.S. Xu, Y.Y. Dang, J.J. Guo, G.S. Wu, J.J. Lu, X.P. Chen, Y.T. Wang, Furanodiene induces endoplasmic reticulum stress and presents antiproliferative activities in lung cancer cells, Evid. Based Complement. Altern. Med. (2012), http://dx.doi.org/10.1155/2012/426521.
[37] A.W. Boots, H. Li, R.P. Schins, R. Duffin, J.W. Heemskerk, A. Bast, G.R. Haenen, The quercetin paradox, Toxicol. Appl. Pharmacol. 222 (2007) 89–96.
[38] S. Son, B.A. Lewis, Free radical scavenging and antioxidative activity of caffeic acid amide and ester analogues: structure-activity relationship, J. Agric. Food Chem. 50 (2002) 468–472.
[39] H. Parlakpinar, S. Tasdemir, A. Polat, A. Bay-Karabulut, N. Vardi, M. Ucar, A. Acet, Protective role of caffeic acid phenethyl ester (cape) on gentamicin-induced acute renal toxicity in rats, Toxicology 207 (2005) 169–177.
[40] P.D. Vivancos, T. Wolff, J. Markovic, F.V. Pallardó, C.H. Foyer, A nuclear glutathione cycle within the cell cycle, Biochem. J. 431 (2010) 169–178.
[41] H. Raza, A. John, S. Benedict, Acetylsalicylic acid-induced oxidative stress, cell cycle arrest, apoptosis and mitochondrial dysfunction in human hepatoma HepG2 cells, Antioxid. Redox Signal. 16 (2012) 1150–1180.
[42] V.G. Antico Arciuc, M.E. Elguero, J.J. Poderoso, M.C. Carreras, Mitochondrial regulation of cell cycle and proliferation, Antioxid. Redox Signal. 16 (2012) 1150–1180.
[43] J.D. Clarke, R.H. Dashwood, E. Ho, Multi-targeted prevention of cancer by sulforaphane, Cancer Lett. 269 (2008) 291–304.
[44] T. Fojo, S. Bates, Strategies for reversing drug resistance, Oncogene 22 (2003) 7512–7523.
[45] D. Del Bufalo, B. Bucci, I. D'Agnano, G. Zupi, N-methylformamide as a potential therapeutic approach in colon cancer, Dis. Colon Rectum 37 (1994) S133–S137.
[46] J.S. Lewis-Wambi, H.R. Kim, C. Wambi, R. Patel, J.R. Pyle, A.J. Klein-Szanto, V. C. Jordan, Buthionine sulfoximine sensitizes antihormone-resistant human breast cancer cells to estrogen-induced apoptosis, Breast Cancer Res. (2008), http://dx.doi.org/10.1186/bcr2208.
[47] H.J. Thibaut, L. van der Linden, P. Jiang, B. Thys, M.D. Canela, L. Aguado, B. Rombaut, E. Wimmer, A. Paul, M.J. Pérez-Pérez, F.J. van Kuppeveld, J. Neyts, Binding of glutathione enterovirus capsids is essential for virion morphogenesis, PLoS Pathog. (2014), http://dx.doi.org/10.1371/journal.ppat.1004039.
[48] M.J. Tisdale, M.B. Mahmoud, Activities of free radical metabolizing enzymes in tumours, Br. J. Cancer 47 (1983) 809–812.